Vol 18 No 5, May 2009
1674-1056/2009/18(05)/2082-14
Chinese Physics B
© 2009 Chin. Phys. Soc.
and IOP Publishing Ltd

Stochasticity in the yeast mating pathway*

Wang Hong-Li(王宏利)[a)b)c)], Fu Zheng-Ping(傅正平)[a)],
Xu Xin-Hang(徐昕航)[a)], and Ouyang Qi(欧阳颀)[a)b)c)†]

[a)] *State Key Laboratory for Mesoscopic Physics, School of Physics, Peking University, Beijing* 100871, *China*
[b)] *The Beijing-Hong Kong-Singapore Joint Center for Nonlinear and Complex Systems (PKU)*
[c)] *Center for Theoretical Biology, Peking University, Beijing* 100871, *China*

(Received 31 July 2008; revised manuscript received 3 September 2008)

We report stochastic simulations of the yeast mating signal transduction pathway. The effects of intrinsic and external noise, the influence of cell-to-cell difference in the pathway capacity, and noise propagation in the pathway have been examined. The stochastic temporal behaviour of the pathway is found to be robust to the influence of inherent fluctuations, and intrinsic noise propagates in the pathway in a uniform pattern when the yeasts are treated with pheromones of different stimulus strengths and of varied fluctuations. In agreement with recent experimental findings, extrinsic noise is found to play a more prominent role than intrinsic noise in the variability of proteins. The occurrence frequency for the reactions in the pathway are also examined and a more compact network is obtained by dropping most of the reactions of least occurrence.

Keywords: noise, stochastic simulation, pheromone response mating pathway of yeast
PACC: 8220F, 8725, 8730E

1. Introduction

The signalling pathway by which yeast *Saccharomyces cerevisiae* responds to a surrounding mating pheromone is a prototypical dynamical network in biochemical reactions. Signal transduction is initiated by binding the mating pheromone to receptors embedded in the plasma membrane, and then a successive biochemical change in the cytoplasm and nucleus starts. The pathway ends up with the fusion of two opposite haploid cells to form a diploid. Extensive experimental studies of genetics, biochemistry, and cell biology have been combined to disclose details of the pathway.[1−5] Mathematically, a few researchers have performed modelling and simulations to analyse the functional and structural characteristics for the components of the pathway.[6−10] Dynamical studies of ordinary differential equations (ODE) of the mass action law for the whole pathway at the system level have also been recently investigated.[11,12]

The proper functions of such a network might be constantly influenced by stochastic fluctuations arising from the inherently random nature of chemical reactions as well as externally from fluctuating reaction rates due to stochastic variations in the global pool of housekeeping genes. The effect of such noise can play a crucial role in biological processes and is the focus of current experimental and theoretical investigations.[13,14] The purpose of this paper is to examine the effects of noise in the yeast mating pathway by direct stochastic simulations of the biochemical kinetics.[12] We distinguish two types of noise, intrinsic noise due to the inherently random nature of reactions in the pathway, and extrinsic noise due to environmental fluctuations and cellular heterogeneities. The effect of both internal and extrinsic noise and their propagations in the pathway can be examined directly.

Our motivation to examine the stochastic process of signal transduction is also aroused by recent experimental work that studied cell-to-cell variations in genetically identical cells. Quantitative results reported from gene expressions[15,16] and in the mating pheromone response pathway in yeast[17] revealed that intrinsic noise contributes little to cell-to-cell variation. Instead, the variation is dominated by extrinsic noise, i.e., differences in the levels of cellular com-

*Project supported by the National Natural Science Foundation of China (Grant No 10774008) and National Key Basic Research Program of China (Grant Nos 2007CB814800 and 2006CB910706). Fu and Xu thank the support of the National Funds for Fostering Talents in Basic Science of China (Grant No J0630311).
†Corresponding author. E-mail: qi@pku.edu.cn

ponents needed for gene expression or differences in the capacity of individual cells to transmit the signal through the pathway. In the framework of stochastic simulations, the contributions of both intrinsic and extrinsic noise to cell-to-cell variation can be directly quantified, and the experimental findings can then be tested directly in our brute force stochastic simulations.

Using Gillespie's algorithm,[18] we examine the stochastic dynamics of the pheromone response of the pathway for an individual or a population of yeast. The effects of inherent and external noise on rate constants and cell-to-cell variation in the pathway capacity and their propagation in the signalling network are checked. The stochastic temporal behaviour of the pathway is found to be robust to inherent fluctuations. Despite the fact that the yeasts are treated with pheromones of very different stimulus strengths and of varied fluctuations, the response fluctuations of protein in the pathway tend to be uniform. The dependence of noise susceptibility on parametric noise strength from stochastic simulations and from Langevin equations are checked. As a confirmation of the recent experimental findings, extrinsic noise is found to play a more prominent role than intrinsic noise in the variability of proteins, and only a small proportion of total cell-to-cell variation is caused by internal random fluctuations. The occurrence frequencies sorted in descending order for the reactions in the pathway are found to show an exponential decay. A more compact network is obtained by dropping most of the reactions of least occurrence.

2. Model and methodology

When a haploid yeast cell of *MAT*a (or *MAT*α) is stimulated by a pheromone of α-factor (or a-factor), it undergoes a series of physiological changes for mating, e.g., changes in gene expressions, cell-cycle arrest in the G_1 phase, oriented growth toward the mating partner (by forming a shmoo tip), and the final fusion of the mating partners. In the following, we summarize the mating signal transduction process for a *MAT*a mutant (TMY101,[9] in which the gene BAR1 whose product can be excreted from the cells and cleave the a-factor is deleted from the wild type) that we consider (see Fig.1 for a simplified spatial diagram for the pathway).

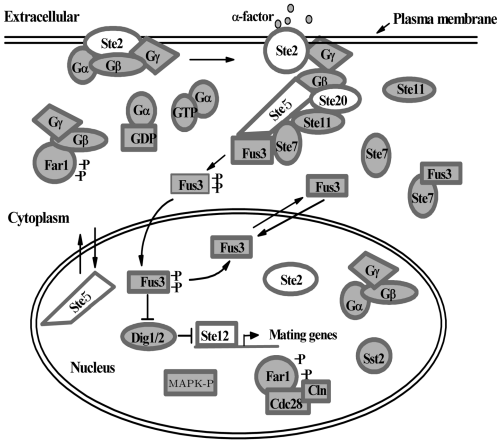


Fig.1. A schematic diagram of the pheromone response pathway in yeast. The pheromone α-factor approaches the receptor Ste2 and stimulates the coupled G protein. The activation of the G protein leads to a series of changes. Gα is dislocated from the G protein, and G$\beta\gamma$ binds to Ste20 and to Ste5. The scaffold protein Ste5 binds to Ste11, Ste7 and Fus3 as elements of the MAPK cascade. Fus3 and Ste5 shuttle between the cytosol and nucleus. The phosphorylated Fus3 may enter the nucleus to inhibit Dig1/2 and activate the transcription factor Ste12 which starts up the expression of mating genes.

The transduction is initiated by binding the α-factor to the receptor Ste2 on the cell surface. The activated Ste2 in turn activates the heterotrimeric G protein that couples to it. The subunit G$\beta\gamma$ is then dislocated from the activated G protein. The signal is subsequently transmitted to the effector proteins Ste20 and scaffold Ste5 that bind to G$\beta\gamma$, resulting in the scaffold-dependent MAPK cascade of four protein kinases: Ste20 phosphorylates and activates Ste11 (MAPKKK), which phosphorylates and activates Ste7 (MAPKK), and Ste7 in turn phosphorylates and activates the Fus3 (MAPK). The cascade is highly dependent on the scaffold protein Ste5 which acts as a platform by providing binding sites for Ste11, Ste7 and Fus3. In parallel, the MAPK cascade can also occur partly in cytosol without the participation of Ste5. Once the MAPK Fus3 is phosphorylated into Fus3pp on the scaffold, it quickly dissociates from Ste5 while the scaffold remains tethered to the plasma membrane. Fus3pp produced from the scaffold and also from the cytosol MAPK cascade travels into the nucleus, and starts the downstream effect. The changes in the nucleus are very complex involving about 200 genes expressed and 100 genes repressed[19] significantly. Generally, Fus3pp phosphorylates and activates the protein Ste12 which is originally repressed. Ste12 is key because it binds to about

100 promoters.[20] The free Ste12 interacts with other proteins of the transcription machinery and thereby activates transcription of many different genes, including expression of the multi-functional regulator Far1. In the nucleus, Far1pp binds to protein Cdc28 to form a Far1pp-Cdc28 complex which promotes arrest of the yeast cell-cycle in the G_1 phase. In cytoplasm, Far1 is phosphorylated and binds to G$\beta\gamma$ to form Far1pp-G$\beta\gamma$. The complex stimulates the polarized growth of the cell towards its mating partner.

A large amount of experimental data and information have been collected about the mechanism, the functioning and the output for the pathway. Crucial components of the pathway such as the G protein cycle,[1,3] the mitogen-activated protein kinase (MAPK) cascade,[1,4] kinase-scaffold proteins,[5] and the order in which they function are well understood. For our stochastic simulations, we here adopt the recently proposed model for the pathway in Ref.[12] which has integrated most of the known essential features of the pathway. Deterministic simulations of a *MAT*a cell exposed to the pheromone α-factor were reported to agree with a wide range of experimental data. In the following, we list all the reactions that we consider in the pathway. As in Ref.[12], all unbound substances in their different phosphorylation states and all complexes are viewed as individual species. Biochemical changes such as complex formations and disintegrations, degradations and phosphorylations or dephosphorylations, and gene expression are considered as reactions at their respective rates. The shuttling of proteins between the cytosol and the nucleus is considered as a reaction, and proteins in the cytosol or in the nucleus are treated as different species and denoted by a subscript out or in. The upstream of the pathway is mainly the G-protein cycle that consists of 10 reactions, i.e., R_i, $i = 1, 2, \ldots, 10$ (the order of the reactions are arranged for index i from forward to backward, and left to right),

$$
\begin{aligned}
&R_1 - R_2 : \mathrm{Ste2} + \alpha - \mathrm{factor} \underset{k_2}{\overset{k_1}{\rightleftharpoons}} \mathrm{Ste2_{active}} \\
&R_3 : \quad \mathrm{Ste2_{active}} \xrightarrow{k_3} \quad \text{(degradation)} \\
&R_4 : \quad \xrightarrow[k_6]{k_4, k_5, \mathrm{ste12a}} \mathrm{Ste2} \quad \text{(synthesis)} \\
&R_5 : \quad \mathrm{Ste2} \xrightarrow{k_7} \\
&R_6 : \quad G \xrightarrow[k_8]{\mathrm{Ste2_{active}}} \mathrm{G}\alpha \cdot \mathrm{GTP} + \mathrm{G}\beta\gamma \\
&R_7 - R_8 : \quad \xrightarrow[k_{11}]{k_9, k_{10}, \mathrm{ste12a}} \mathrm{G} \xrightarrow{k_{12}} \\
&R_9 : \quad \mathrm{G}\alpha \cdot \mathrm{GTP} \xrightarrow[\mathrm{Sst2_{active}}, k_{14}]{k_{13}} \mathrm{G}\alpha \cdot \mathrm{GDP} \\
&R_{10} : \quad \mathrm{G}\alpha \cdot \mathrm{GDP} + \mathrm{G}\beta\gamma \xrightarrow{k_{15}} \mathrm{G},
\end{aligned}
$$

where k_i are the reaction rates, and the protein above or below the arrow is the enzyme or transcription factor of the reaction which can be described with a Hill function. The scaffold protein Ste5 is located initially in the nucleus and is recruited to the shmoo tip after the cell is activated by the pheromone. This involves the following R_{11}–R_{20} reactions,

$$
\begin{aligned}
&R_{11} - R_{12} : \quad \mathrm{G}\beta\gamma + \mathrm{Ste5_{out}} \underset{k_{17}}{\overset{k_{16}}{\rightleftharpoons}} \mathrm{G}\beta\gamma.\mathrm{Ste5_{out}} \\
&R_{13} - R_{14} : \quad \mathrm{Ste20} + \mathrm{G}\beta\gamma \cdot \mathrm{Ste5_{out}} \underset{k_{19}}{\overset{k_{18}}{\rightleftharpoons}} \mathrm{C1} \\
&R_{15} - R_{16} : \quad \mathrm{G}\beta\gamma + \mathrm{Ste20} \underset{k_{19}}{\overset{k_{18}}{\rightleftharpoons}} \mathrm{G}\beta\gamma.\mathrm{Ste20} \\
&R_{17} - R_{18} : \quad \mathrm{Ste5_{out}} + \mathrm{G}\beta\gamma \cdot \mathrm{Ste20} \underset{k_{17}}{\overset{k_{16}}{\rightleftharpoons}} \mathrm{C1} \\
&R_{19} - R_{20} : \quad \mathrm{Ste5_{in}} \underset{k_{23}}{\overset{k_{22}}{\rightleftharpoons}} \mathrm{Ste5_{out}}.
\end{aligned}
$$

The MAPK cascade involving the elements Ste11, Ste7 and Fus3 can occur in the cytosol. These have 34 reactions of phosphorylation and dephosphorylation,

$$
\begin{aligned}
&R_{21} - R_{23} : \quad \mathrm{Ste11p} + \mathrm{MAPKKK-P} \rightleftharpoons \mathrm{Ste11pMAPKKK-P} \rightarrow \mathrm{Ste11} + \mathrm{MAPKKK-P} \\
&R_{24} - R_{26} : \quad \mathrm{Ste11pp} + \mathrm{MAPKKK-P} \rightleftharpoons \mathrm{Ste11ppMAPKKK-P} \rightarrow \mathrm{Ste11p} + \mathrm{MAPKKK-P} \\
&R_{27} - R_{29} : \quad \mathrm{Ste11pp} + \mathrm{Ste7} \rightleftharpoons \mathrm{Ste11ppSte7} \rightarrow \mathrm{Ste11pp} + \mathrm{Ste7p} \\
&R_{30} - R_{32} : \quad \mathrm{Ste7p} + \mathrm{MAPKK-P} \rightleftharpoons \mathrm{Ste7pMAPKK-P} \rightarrow \mathrm{Ste7} + \mathrm{MAPKK-P} \\
&R_{33} - R_{35} : \quad \mathrm{Ste11pp} + \mathrm{Ste7p} \rightleftharpoons \mathrm{Ste11ppSte7p} \rightarrow \mathrm{Ste11pp} + \mathrm{Ste7pp} \\
&R_{36} - R_{38} : \quad \mathrm{Ste7pp} + \mathrm{MAPKK-P} \rightleftharpoons \mathrm{Ste7ppMAPKK-P} \rightarrow \mathrm{Ste7p} + \mathrm{MAPKK-P} \\
&R_{39} - R_{41} : \quad \mathrm{Ste7pp} + \mathrm{Fus3} \rightleftharpoons \mathrm{Ste7ppFus3} \rightarrow \mathrm{Ste7pp} + \mathrm{Fus3p}
\end{aligned}
$$

$$R_{42}-R_{44}: \quad \mathrm{Fus3p}+\mathrm{MAPK}-\mathrm{P}_{\mathrm{out}} \rightleftharpoons \mathrm{Fus3pMAPK}-\mathrm{P} \rightarrow \mathrm{Fus3}+\mathrm{MAPK}-\mathrm{P}_{\mathrm{out}}$$

$$R_{45}-R_{47}: \quad \mathrm{Ste7pp}+\mathrm{Fus3p} \rightleftharpoons \mathrm{Ste7ppFus3p} \rightarrow \mathrm{Ste7pp}+\mathrm{Fus3pp}_{\mathrm{out}}$$

$$R_{48}-R_{50}: \quad \mathrm{Fus3pp}_{\mathrm{out}}+\mathrm{MAPK}-\mathrm{P}_{\mathrm{out}} \rightleftharpoons \mathrm{Fus3ppMAPK}-\mathrm{P} \rightarrow \mathrm{Fus3p}+\mathrm{MAPK}-\mathrm{P}_{\mathrm{out}}$$

$$R_{51}-R_{52}: \quad \mathrm{Ste7}+\mathrm{Fus3}_{\mathrm{out}} \underset{k_{25}}{\overset{k_{24}}{\rightleftharpoons}} \mathrm{Ste7}\cdot\mathrm{Fus3}_{\mathrm{out}}$$

$$R_{53}: \quad \mathrm{Ste11} \xrightarrow{k_{26},\mathrm{Fus3pp}}$$

$$R_{54}: \quad \mathrm{Ste7pp} \xrightarrow{k_{27}},$$

where '–P' denotes dephosphorylation kinases. The MAPK cascade occurs mainly on the scaffold. All possible scaffold–kinase complex C_i (see Appendix) with MAPK elements and cascade changes are considered, involving 105 reactions,

$$\begin{array}{lll}
R_{55}-R_{60}: & C_1+\mathrm{Ste11} \rightleftharpoons C_2 & C_1+\mathrm{Ste11pp} \rightleftharpoons C_3 \quad C_1+\mathrm{Ste7} \rightleftharpoons C_4 \\
R_{61}-R_{64}: & C_1+\mathrm{Ste7pp} \leftarrow C_5 & C_1+\mathrm{Fus3} \rightleftharpoons C_6 \quad C_1+\mathrm{Fus3pp} \leftarrow C_7 \\
R_{65}-R_{68}: & C_2 \rightarrow C_3 & C_2+\mathrm{Ste7} \rightleftharpoons C_8 \quad C_2+\mathrm{Ste7pp} \leftarrow C_{11} \\
R_{69}-R_{73}: & C_2+\mathrm{Fus3} \rightleftharpoons C_{12} & C_2+\mathrm{Fus3pp} \leftarrow C_{15} \quad C_3+\mathrm{Ste7} \rightleftharpoons C_9 \\
R_{74}-R_{77}: & C_3+\mathrm{Ste7pp} \leftarrow C_{10} & C_3+\mathrm{Fus3} \rightleftharpoons C_{13} \quad C_3+\mathrm{Fus3pp} \leftarrow C_{14} \\
R_{78}-R_{83}: & C_4+\mathrm{Ste11} \rightleftharpoons C_8 & C_4+\mathrm{Ste11pp} \rightleftharpoons C_9 \quad C_4+\mathrm{Fus3} \rightleftharpoons C_{16} \\
R_{84}-R_{88}: & C_4+\mathrm{Fus3pp} \leftarrow C_{19} & C_5+\mathrm{Fus3pp} \rightleftharpoons C_{10} \quad C_5+\mathrm{Ste11} \rightleftharpoons C_{11} \\
R_{89}-R_{93}: & C_5+\mathrm{Fus3} \rightleftharpoons C_{17} & C_5+\mathrm{Fus3pp} \leftarrow C_{18} \quad C_6+\mathrm{Ste11} \rightleftharpoons C_{12} \\
R_{94}-R_{98}: & C_6+\mathrm{Ste11pp} \rightleftharpoons C_{13} & C_6+\mathrm{Ste7} \rightleftharpoons C_{16} \quad C_6+\mathrm{Ste7pp} \leftarrow C_{17} \\
R_{99}-R_{103}: & C_7+\mathrm{Ste11pp} \rightleftharpoons C_{14} & C_7+\mathrm{Ste11} \rightleftharpoons C_{15} \quad C_7+\mathrm{Ste7pp} \leftarrow C_{18} \\
R_{104}-R_{108}: & C_7+\mathrm{Ste7} \rightleftharpoons C_{19} & C_8 \rightarrow C_9 \quad C_8+\mathrm{Fus3} \rightleftharpoons C_{20} \\
R_{109}-R_{112}: & C_8+\mathrm{Fus3pp} \leftarrow C_{23} & C_9 \rightarrow C_{10} \quad C_9+\mathrm{Fus3} \rightleftharpoons C_{21} \\
R_{113}-R_{116}: & C_9+\mathrm{Fus3pp} \leftarrow C_{25} & C_{10} \leftarrow C_{11} \quad C_{10}+\mathrm{Fus3} \rightleftharpoons C_{24} \\
R_{117}-R_{120}: & C_{10}+\mathrm{Fus3pp} \leftarrow C_{27} & C_{11}+\mathrm{Fus3} \rightleftharpoons C_{22} \quad C_{11}+\mathrm{Fus3pp} \leftarrow C_{26} \\
R_{121}-R_{124}: & C_{12} \rightarrow C_{13} & C_{12}+\mathrm{Ste7} \rightleftharpoons C_{20} \quad C_{12}+\mathrm{Ste7pp} \leftarrow C_{22} \\
R_{125}-R_{128}: & C_{13}+\mathrm{Ste7} \rightleftharpoons C_{21} & C_{13}+\mathrm{Ste7pp} \leftarrow C_{24} \quad C_{14} \leftarrow C_{15} \\
R_{129}-R_{133}: & C_{14}+\mathrm{Ste7} \rightleftharpoons C_{25} & C_{14}+\mathrm{Ste7pp} \leftarrow C_{27} \quad C_{15}+\mathrm{Ste7} \rightleftharpoons C_{23} \\
R_{134}-R_{138}: & C_{15}+\mathrm{Ste7pp} \leftarrow C_{26} & C_{16}+\mathrm{Ste11pp} \rightleftharpoons C_{21} \quad C_{16}+\mathrm{Ste11} \rightleftharpoons C_{20} \\
R_{139}-R_{143}: & C_{17} \rightarrow C_{18} & C_{17}+\mathrm{Ste11pp} \rightleftharpoons C_{24} \quad C_{17}+\mathrm{Ste11} \rightleftharpoons C_{22} \\
R_{144}-R_{149}: & C_{18}+\mathrm{Ste11pp} \rightleftharpoons C_{27} & C_{18}+\mathrm{Ste11} \rightleftharpoons C_{26} \quad C_{19}+\mathrm{Ste11pp} \rightleftharpoons C_{25} \\
R_{150}-R_{153}: & C_{19}+\mathrm{Ste11} \rightleftharpoons C_{23} & C_{20} \rightarrow C_{21} \quad C_{21} \rightarrow C_{24} \\
R_{154}-R_{156}: & C_{22} \rightarrow C_{24} & C_{22} \rightarrow C_{26} \quad C_{23} \rightarrow C_{25} \\
R_{157}-R_{159}: & C_{24} \rightarrow C_{27} & C_{25} \rightarrow C_{27} \quad C_{26} \rightarrow C_{27}.
\end{array}$$

The downstream of the pathway that occurs in the nucleus is a complex network involving many regulatory factors and expressions of many mating-genes. Following Ref.[12], we consider here a simplification of the real processes. When Fus3pp enters into the nucleus, we consider the following 26 reactions,

$$R_{160}-R_{161}: \quad \underset{k_{30}}{\overset{\mathrm{Fus3pp}_{\mathrm{in}},k_{28},k_{29}}{\rightleftharpoons}} \mathrm{Ste12}_{\mathrm{active}}$$

$$R_{162}: \quad \xrightarrow{\mathrm{Ste12}_{\mathrm{active}},k_{31},k_5} \mathrm{MAPK}-\mathrm{P}_{\mathrm{in}}$$

$$R_{163}: \quad \xrightarrow{\mathrm{Ste12a,k32,k5}} \mathrm{Fus3}$$

$$R_{164}-R_{169}: \quad \underset{k_{35}}{\overset{\mathrm{Ste12_{active}},k_{33},k_{34}}{\rightleftharpoons}} \mathrm{Far1_{in}} \underset{k_{37}}{\overset{\mathrm{Fus3pp_{in}},k_{36}}{\rightleftharpoons}} \mathrm{Far1pp_{in}} \underset{k_{39}}{\overset{k_{38}}{\rightleftharpoons}} \mathrm{Far1pp_{out}}$$

$$R_{170}-R_{171}: \quad \mathrm{Far1pp_{out}} + \mathrm{G}\beta\gamma \underset{k_{41}}{\overset{k_{40}}{\rightleftharpoons}} \mathrm{Far1ppG}\beta\gamma$$

$$R_{172}-R_{173}: \quad \mathrm{Far1pp_{in}} + \mathrm{Cdc28} \underset{k_{43}}{\overset{k_{42}}{\rightleftharpoons}} \mathrm{Far1ppCdc28}$$

$$R_{174}-R_{175}: \quad \underset{k_{46}}{\overset{\mathrm{Ste12_{active}},k_{44},k_{45}}{\rightleftharpoons}} \mathrm{Sst2_{active}}$$

$$R_{176}-R_{178}: \quad \mathrm{Fus3pp_{in}} + \mathrm{MAPK-P_{in}} \rightleftharpoons \mathrm{Fus3ppMAPK-P_{in}} \quad \rightarrow \mathrm{Fus3p_{in}} + \mathrm{MAPK-P_{in}}$$

$$R_{179}-R_{181}: \quad \mathrm{Fus3p_{in}} + \mathrm{MAPK-P_{in}} \rightleftharpoons \mathrm{Fus3pMAPK-P_{in}} \rightarrow \mathrm{Fus3_{in}} + \mathrm{MAPK-P_{in}}$$

$$R_{182}-R_{183}: \quad \mathrm{Fus3_{in}} \underset{48}{\overset{k_{47}}{\rightleftharpoons}} \mathrm{Fus3_{out}}$$

$$R_{184}-R_{185}: \quad \mathrm{Fus3pp_{in}} \underset{k_{50}}{\overset{k_{49}}{\rightleftharpoons}} \mathrm{Fus3pp_{out}}$$

The above biochemical changes in the pathway form a complex reaction network which consists of 185 reaction steps and involves 76 proteins and substrates. For simplicity, the cytosol is restricted to the shmoo tip because it is where many signalling proteins are concentrated and is the main place for the upstream reactions, including the reactions involving G protein and Ste5 scaffold. As in Ref.[12], the model involves two physical locations, i.e., the shmoo tip and the nucleus between which proteins such as Ste5, Fus3 or Fus3pp, and Far1 shuttle. The network we consider here is slightly different from that in Ref.[12], i.e., we do not take into account the reactions involving Ste5 in cytosol because our deterministic simulations show that including these reactions does not affect significantly the temporal features as well as other properties of the pathway.

As deterministic behaviour in this model has been investigated,[12] here we carry out direct stochastic simulations of the above reactions by using Gillespie's method in Ref.[18]. To achieve speedup for the simulation, we adopt the accelerated algorithm known as the K-level scheme[21] where the data structure for the reaction channels is organized into a binary tree. The reaction constants used in the stochastic simulation are determined from the macroscopic reaction rates adopted in Ref.[12], i.e., a macroscopic rate with dimension factor $(nM)^n$ is multiplied by the factor $\Omega \equiv (10^{-9} \times N_{\mathrm{A}} V)^n$, where nM is nanomole, n is an integer, and N_{A} the Avogadro constant. V is the effective volume of the cell, which could be smaller than the yeast cell volume (about 6.5×10^{-14} L) because the proteins and substrates are spatially restricted. Based on experimental data,[8] we estimate the value of Ω to be about 8.0 with $V = 1.33 \times 10^{-14}$ L. Ω is also the population scale for the species and measures the intrinsic molecular fluctuation with smaller values corresponding to more intensive intrinsic noise. By tuning Ω, the intensity of the intrinsic noise can be adjusted.

In order to demonstrate the dynamical behaviour of the pathway, we select several key proteins or complexes in the modules of the pathway as the representation of the integer feature of the pathway. These include, in the temporal order of their functions in the signal transduction, activated G protein and the complex Ste20·G$\beta\gamma$ in the G protein cycle, activated Ste5, Ste11pp and Fus3pp in the Ste5-related module and in the MAPK cascade, and key species in the downstream of the pathway, i.e., activated Ste12, Far1ppCdc28 and Far1ppG$\beta\gamma$.

The reaction parameters and initial protein concentrations in the model were derived from experiments whenever possible and estimated according to the mechanisms and similar reactions in other organisms.[12] In all our simulations, the pathway before being activated by the pheromone lies in the rest state where some species adopt their constant concentrations while other proteins or complexes have zero copy. All the reaction rates and initial concentrations are fixed, or otherwise follow individually normal distributions when the pathway is simulated for a population of yeast. We list the model parameter values and initial concentrations in the Appendix.

3. Results

3.1. Intrinsic noise

We first examine the effect of pure intrinsic noise in the signalling pathway. The intensity of the inherent noise is adjusted by tuning Ω. Figure 2 demonstrates the simulated results. The time variations of eight key proteins selected from the pathway are depicted. The results are generated by treating persistently the yeast with α-factor of constant concentration 1000 nM (about 8000 copies with $\Omega = 8.0$). As Ω is decreased from 8.0, to 1.0 and to 0.1, the copy number of the protein becomes lower and lower and the noise intensity grows. At $\Omega = 0.1$, some species in the pathway have only several copies. In Fig.2, despite very different intensities of noise, the temporal variations of concentration overlap with each other. Strong intrinsic noise generally makes the trajectories more dithering. Under the influence of inherent noise, the response pattern of the pathway is conservative and the function of the pathway is therefore robust to intrinsic noise. Figure 2 also shows that the intrinsic noise is most drastic in the MAPK cascade where Ste11 and Fus3 are phosphorylated to Ste11pp and Fus3pp. The above observation does not rely on the pheromone concentration, and similar results are obtained when the system is treated with a different amount of α-factor.

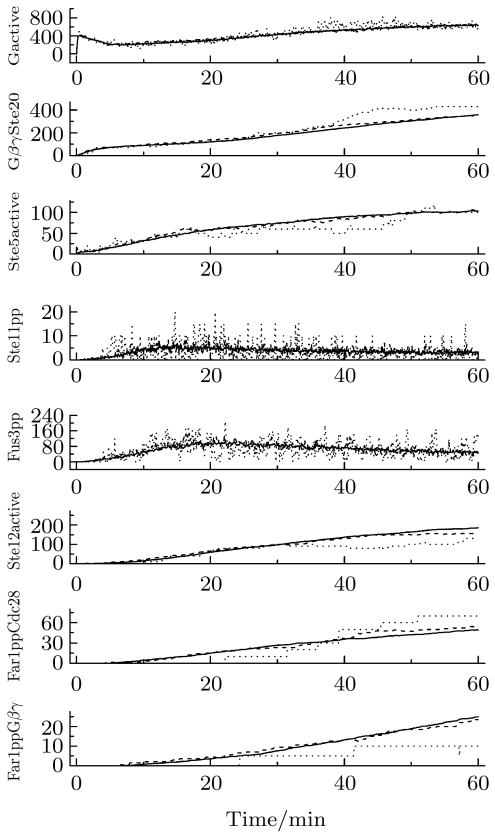


Fig.2. Effect of intrinsic noise of different intensity (different Ω) on the signal transduction process. From top to bottom, the curves are the temporal variations of eight key species, i.e. , activated G protein, the binding of Ste20 to G$\beta\gamma$, activation of the scaffold Ste5, Ste11pp, Fus3pp, active Ste12, Far1ppCdc28 and Far1ppG$\beta\gamma$, in the order of their successive activation in the pathway. Parameters: $\Omega = 0.1$ for dotted lines; $\Omega = 1$ for dashed lines; $\Omega = 8$ for solid lines.

We next consider a population of 200 completely identical yeast cells (identical not only genetically but also in the concentrations and states of their cellular components), and perform 200 stochastic simulation runs of the signal transduction. The time evolution varies from cell to cell due to the influence of inherent stochasticity or intrinsic noise whose strength can be evaluated by the variation in the level of protein. We adopt the relative standard deviation (RSD) as a measure of the variation in the amount of protein, i.e. ,

$$\eta \equiv \sqrt{\langle x^2 \rangle - \langle x \rangle^2} / \langle x \rangle. \tag{1}$$

Here η is a function of time as species x is dependent on time. Throughout this paper, values of η for the key species are calculated as their abundances grow approximately to their maxima or to sufficiently high values from the simulation runs, i.e. , for the activated G protein at 5 minutes, G$\beta\gamma$ Ste20 complex at 10 minutes, Ste11pp at 15 minutes, Ste7pp and Fus3pp at 20 minutes, and activated Ste12, Far1ppCdc28, and Far1ppG$\beta\gamma$ at 40 minutes, in the temporal order of their functions in the pathway.

Figure 3 (black columns) demonstrates the values of η for the key proteins in the pathway when the yeasts are treated identically with α-factor of 1000 nM and simulated with identical initial conditions. As there is no extrinsic noise that affects the signal transduction, η measures the strength of pure intrinsic noise. For a much lower stimulus strength with α-factor = 20 nM, the results are depicted in Fig.3 (grey columns) and have been obtained similarly from 200 simulation runs with the same initial condition. Despite the fact that the activation strength is very different, the pattern of η for the key species with α-factor = 20 nM differs little from that with α-factor = 1000 nM.

The yeasts have been so far treated uniformly with identical α-factor concentrations. To examine

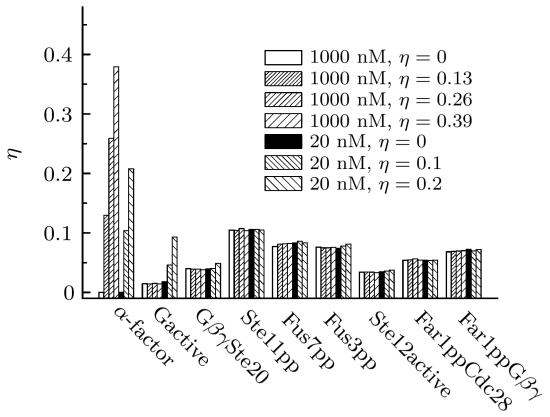


Fig.3. Intrinsic noise in the selected key proteins from the upstream (activated G-protein, G$\beta\gamma$Ste20) to the downstream (Fus3pp$_{\rm out}$, active Ste12, FarppG$\beta\gamma$) of the signal pathway when activated by pheromone of different concentrations (20 nM or 1000 nM) and different fluctuation intensities η. The noise η for the key proteins are obtained from statistics over 200 stochastic simulation runs (see the text for detail).

the effect of fluctuations in the stimulus, we have checked the case where the amounts of pheromone for individual yeasts follow a normal distribution with a mean and relative deviation η. Figure 3 shows the results with varied input noise strengths $\eta = 0.13$, 0.26, and 0.39 with mean α-factor = 1000 nM, or $\eta = 0.1$ and 0.2 with mean α-factor = 20 nM, respectively. We see that the initially aroused noise by the pheromone fades fast as the signal is transmitted down the pathway. Despite the very different mean pheromone concentrations and varied fluctuation strengths, the values of η for the key species in the MAPK cascade and the downstream are approximately identical. The results suggest that the pathway adopts a uniform and robust noise pattern when the system is influenced purely by intrinsic fluctuations.

3.2. Effects of parametric noises and variation in the pathway capacity

We next incorporate external noise and cellular heterogeneity (or cell-to-cell difference) into the pathway. Similar to the above simulations, a population of 200 yeasts is simulated with noisy reaction rates or when the yeasts are different from one another in the capacity of the pathway. The capacity is the ability for the pathway to transduce the mating signal which is dependent on crucial components of the pathway such as Ste2, G protein, Ste20, Ste5, Ste11, Ste7, Fus3, and kinases of MAPKKK-P, MMAPKK-P, and MAPK-P. The amounts of these components (and their locations) determine and represent the capacity of the pathway for signal transduction. Variations in the reaction rates and in the protein amounts for pathway capacity are considered extrinsic noise and can induce additional variations in the level of protein.

We check when parameters are disturbed by noise. The values of the varied rate are selected randomly for the population from a normal distribution with mean $\langle k\rangle$ and RSD $\eta_{\rm p}$. The parametric noise strength is measured by $\eta_{\rm p}$. The conditions for all the simulation runs are identical except for the varied parameter. Figure 4 demonstrates the values of η for the key species when a few reaction rates are individually perturbed by an external Gaussian white noise. The normally distributed noisy rates has a noise strength $\eta_{\rm p} = 0.1$. Figure 4 reveals that externally perturbing some rates, such as off$_{2k}$, k_8, or a_{2k}, can bring significant changes in the fluctuations of the key proteins as compared to those when only the intrinsic noise takes effect (grey columns). The drastic change is a local effect of the perturbed reaction rate. For instance, perturbing off$_{2k}$, the rate at which Fus3pp breaks away from the scaffold Ste5, causes directly a drastic growth in the variation of Fus3pp (see Fig.4). The intensive noise in Fus3pp propagates to the next reaction which is catalyzed by Fus3pp to produce active Ste12 (R_{160}), and results in enhanced variation in Ste12$_{\rm active}$. The influence of the perturbation declines fast and causes no further significant changes in the

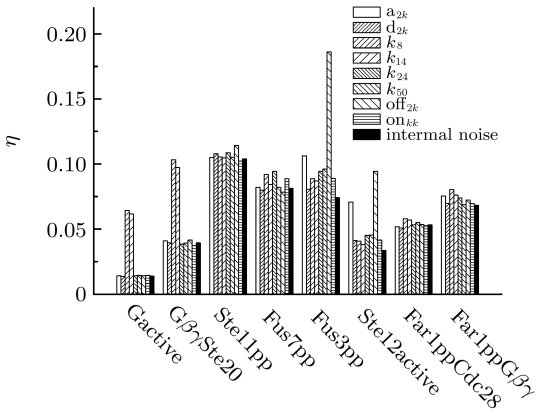


Fig.4. The variation η for the key proteins when an individual rate is perturbed by an external Gaussian white noise. The results are obtained from 200 simulation runs similar to Fig.3. Pure internal noises are represented by the grey columns. Parameters: $\Omega = 4.0$, α-factor = 20 nM. The noisy rates have a uniform noise strength $\eta_{\rm p} = 0.1$.

reactions that are located farther away from the reactions that are perturbed. The local effect is also evident from the columns for k_8, the rate at which G protein is activated to form Gα.GTP and G$\beta\gamma$ (R_6), where the perturbed reaction is located in the upstream of the pathway. It causes only local enhancement of variations in the activated G protein and the complex G$\beta\gamma$·Ste20 (R_{15}).

Effects of stochastic variation in the pathway capacity are also simulated. Generally, the variation in the capacity causes also local effects, mainly bringing on significant noise enhancement in the key proteins involved in the MAPK cascade. For instance, the noisy abundance of Ste11 causes only a burst in η for Ste11pp. Perturbation of Ste5 has aroused the noise enhancement in a broader range of proteins such as Ste7pp, Fus3pp, and activated Ste12. This is because Ste5 is the scaffold and perturbing it can affect all the scaffold-dependent reactions.

Increasing Ω or the activation strength generally decreases the variation strength in the crucial proteins such as Fus3pp, activated Ste12, and Far1ppCdc2. We also checked the results of the corresponding Langevin equations, i.e., ODE rate equations with noisy rate constants, obtained in parallel and the transduction is only influenced by extrinsic noise. Comparison with the direct stochastic simulation reveals that the joint action of extrinsic and intrinsic noise greatly enhances the protein variations.

When a parameter is perturbed by noise, its effect propagates in the pathway. The amplification or attenuation of the parametric noise by the system can be quantitatively estimated by the extrinsic noise susceptibility χ defined as in Ref.[22]

$$\chi = \eta/\eta_{\rm p}, \tag{2}$$

where $\eta_{\rm p}$ is the relative strength of parametric noise in reaction rates or in the pathway capacity, and η is the variation strength of the protein. The dependence of χ on the extrinsic noise strength $\eta_{\rm p}$ has been calculated from stochastic simulations. We observe that the extrinsic noise susceptibility is decreased monotonically as the perturbing noise strength grows. At low values of $\eta_{\rm p}$ the external noise is amplified for $\chi > 1.0$, while it is attenuated at higher strength of noise. Figure 5 depicts the $\chi - \eta_{\rm p}$ curves when the cells are different from one another at all the reaction rates and all the initial amounts of proteins, and have a uniform noise strength $\eta_{\rm p}$. Compared with the results generated in parallel from the Langevin equation, the noise susceptibility of the system is significantly enhanced by the joint influence of extrinsic and intrinsic noise from stochastic simulations.

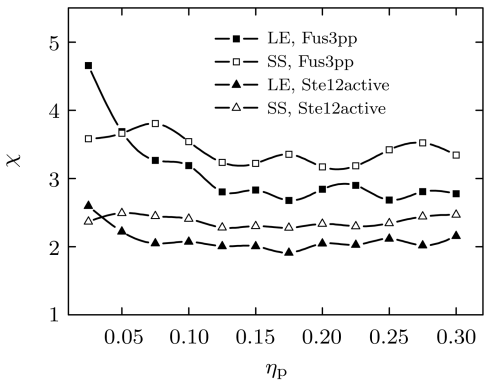


Fig.5. The χ–$\eta_{\rm p}$ dependence calculated when all the reaction rates and all the initial levels of proteins of pathway capacity follow normal distributions with uniform deviations $\eta_{\rm p}$. Parameter: $\Omega = 4.0$, α-factor = 20 nM.

3.3. Roles of intrinsic and extrinsic noise in cell-to-cell variation

In the above, we did not separate the intrinsic and extrinsic contributions to the total variation in the level of proteins in the pathway and the roles of these two types of noise in the cell-to-cell variation are not distinguished. In experiments, the dual-reporter technique has been invented to discriminate these two types of noise in gene expressions,[23] where cyan and yellow fluorescent reporter proteins are expressed from identical promoters at homologous loci. In order to evaluate their respective contributions to or relative portions in cell-to-cell variation, we apply here an analogue of the experimental technique in our simulations.

As protein Far1 plays key roles in the control of the cell cycle arrest in the G_1 phase and is involved in polarized growth of the cell, reactions related to Far1, i.e., $R_{164} - R_{173}$, represent a main part of the downstream effect of the pathway. Analogous to the cyan and yellow fluorescent reporter proteins implemented in experiments, we suppose that Far1 or as a component of complexes in reactions $R_{164} - R_{173}$ has two types of 'colours' labelled 'A' and 'B'. The same species with different color are chemically identical, and they react as follows,

$$R_{164}-R_{169}: \overset{\mathrm{Ste12_{active}},k_{33},k_{34}}{\underset{k_{35}}{\rightleftharpoons}} \mathrm{Far1_{in}-A} \overset{\mathrm{Fus3pp_{in}},k_{36}}{\underset{k_{37}}{\rightleftharpoons}} \mathrm{Far1pp_{in}-A} \overset{k_{38}}{\underset{k_{39}}{\rightleftharpoons}} \mathrm{Far1pp_{out}-A}$$

$$R_{170}-R_{171}: \mathrm{Far1pp_{out}-A+G}\beta\gamma \overset{k_{40}}{\underset{k_{41}}{\rightleftharpoons}} \mathrm{Far1ppG}\beta\gamma-\mathrm{A}$$

$$R_{172}-R_{173}: \mathrm{Far1pp_{in}-A+Cdc28} \overset{k_{42}}{\underset{k_{43}}{\rightleftharpoons}} \mathrm{Far1ppCdc28-A}$$

$$R'_{164}-R'_{169}: \overset{\mathrm{Ste12_{active}},k_{33},k_{34}}{\underset{k_{35}}{\rightleftharpoons}} \mathrm{Far1_{in}-B} \overset{\mathrm{Fus3pp_{in}},k_{36}}{\underset{k_{37}}{\rightleftharpoons}} \mathrm{Far1pp_{in}-B} \overset{k_{38}}{\underset{k_{39}}{\rightleftharpoons}} \mathrm{Far1pp_{out}-B}$$

$$R'_{170}-R'_{171}: \mathrm{Far1pp_{out}-B+G}\beta\gamma \overset{k_{40}}{\underset{k_{41}}{\rightleftharpoons}} \mathrm{Far1ppG}\beta\gamma-\mathrm{B}$$

$$R'_{172}-R'_{173}: \mathrm{Far1pp_{in}-B+Cdc28} \overset{k_{42}}{\underset{k_{43}}{\rightleftharpoons}} \mathrm{Far1ppCdc28-B}.$$

The reactions are hypothetical and are invented just for the decomposition of these two types of noise. Similar to the fluorescent reporter proteins applied in experiments, the products of the duplicated reactions such as Far1ppCdc28 and Far1ppG$\beta\gamma$ can be implemented as reporters. The above reactions for the species of different colours are regulated identically by the upriver Fus3pp and activated Ste12. Variations in these regulators and in the reaction rates, i.e., $k_{33} \sim k_{43}$, provide a fluctuating environment for the above reactions and are the sources of extrinsic noise. The intrinsic noise comes from the inherently random nature of the reactions. We perform stochastic simulations of the modified model that has incorporated the above reactions for a population of yeasts with cellular heterogeneity. From simulation data, intrinsic and extrinsic noise in the reporters can be separated by plots of protein-A versus protein-B amounts in individual cells.[23] Intrinsic noise η_{int} and extrinsic noise η_{ext} have orthogonal contributions to the total η_{tot} and satisfy the relation $\eta_{\mathrm{int}}^2+\eta_{\mathrm{ext}}^2=\eta_{\mathrm{tot}}^2$. As has been elucidated in Ref.[23], the spread of points perpendicular to the diagonal line on which abundances of protein-A and protein-B are equal corresponds to intrinsic noise, whereas the spread parallel to this line is due to extrinsic noise. The total variation in the level of a given protein can be readily decomposed into its intrinsic and extrinsic components.

Figure 6 demonstrates Far1ppCdc28-A versus Far1ppCdc28-B amounts when the population is heterogeneous in the pathway capacity and all other conditions are identical for the stochastic simulation runs. When the pathway capacity is homogeneous in the population (plus), the intrinsic contribution to the total amount of variation in Far1ppCdc28 approaches that of extrinsic noise, with $\eta_{\mathrm{int}}^2 \approx 0.0195$ and $\eta_{\mathrm{ext}}^2 \approx 0.0228$. As the inhomogeneity is turned on with initially distributed proteins in the pathway, the portion of extrinsic noise is increased (see circles and squares in Fig.6) and the spread of points on the diagonal line is significantly enhanced. We see that η_{ext}^2 is about 0.0395 as the variation in the initial proteins $\eta_{\mathrm{p}}=0.1$, and it grows to 0.15 with $\eta_{\mathrm{p}}=0.25$. The portion of intrinsic noise is approximately unchanged. The contribution of extrinsic noise is amplified by the enhanced fluctuations in Fus3pp and active Ste12 that regulate the above Far1-involved reactions. We also

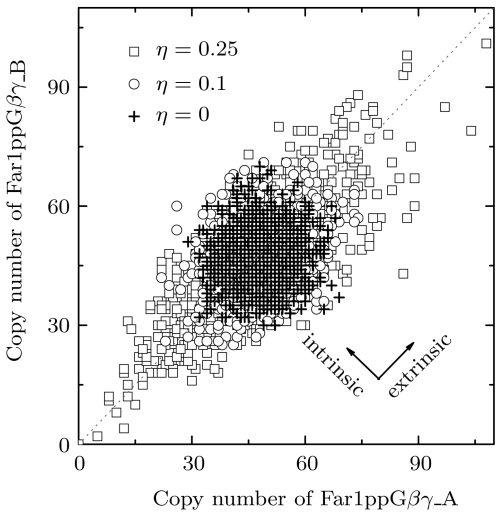


Fig.6. Separation of extrinsic noise and intrinsic noise. The results were obtained by performing 1000 simulation runs when all the initial proteins of pathway capacity follow normal distributions with a uniform deviation η. A dot in the plot represents the amount of Far1ppCdc28_A and Far1ppCdc28_B in an individual yeast in the population. The variation in the copy number of Far1ppG$\beta\gamma$ along the diagonal line grows from 52.5, 91.1, to 348.5 as η changes from 0.0 (plus), 0.1 (circles), to 0.25 (squares). The variation perpendicular to the diagonal line is primarily fixed around 45. Parameters: $\Omega=4$, α-factor = 20 nM.

carried out simulation runs when there were also inhomogeneities in the reaction rates. The component of extrinsic noise in the total variation of the reporter was even more drastically increased. Under the joint influence of the homogeneities in the pathway capacity and in the reaction rates, a small amount of noise can induce significant growth in $\eta^2_{\rm ext}$ for Far1ppG$\beta\gamma$, while the amount of $\eta^2_{\rm int}$ changes little.

Our results suggest that due to the inhomogeneity in the yeast population, the difference in the pathway capacity of individual cells plays a more prominent role than the intrinsic noise in cell-to-cell variation. Extrinsic noise and cellular inhomogeneity have a more important influence than intrinsic noise on the cell-to-cell variation. Stochasticity in the mating pheromone response pathway of yeast has been also studied in a recent *in vivo* experiment.[17] The contributions of intrinsic and extrinsic noise in the total cell-to-cell variation were dissected and measured quantitatively. As we observed in our stochastic simulations, the experimental result revealed that only a small proportion of the total variation is due to intrinsic noise.

3.4. Occurrence frequency of reaction in the pathway

The stochastic simulation approach selects randomly the reaction that occurs next according to the propensity functions of the reactions in the pathway. When the simulation is performed, one can take count of the firing times for each reaction channel in the pathway during the period of the signal transduction. Figure 7(a) shows the firing frequencies for the reactions in the pathway. The data are obtained from a simulation run of the pathway in the period of an hour after the pathway is activated. We see that the frequencies, which have been normalized and are sorted in descending order, fall exponentially. The reactions in the pathway are drastically different in their occurrences. Some reactions such as those in the G-protein cycle (R_6, R_9, R_{10}) and the shuttle of Fus3 and Fus3pp, $R_{182} - R_{185}$, between the cytosol and the nucleus occur most often, while the dissociation of the complex G$\beta\gamma$Ste20 (R_{16}) and the combination of Ste20 with G$\beta\gamma$Ste5 (R_{13}) occur rarely. Under the constant stimuli of the pheromone and activation of receptor Ste2, i.e., R_1, R_2, the G protein is activated frequently, and provides a driving force for the signal transduction. The most frequently fired reactions also include the dephosphorylation of Fus3p or Fus3pp in cytosol and in the nucleus, a few scaffold-dependent reactions (R_{115}, R_{117}, R_{157}), and the forming and decomposition of the complex Ste7·Fus3 (R_{51}, R_{52}). The pattern of firing frequency for the pathway is conservative when the yeast is treated with varied stimulus strengths of pheromone or when the transduction is simulated with different Ω for varied strengths of intrinsic noise.

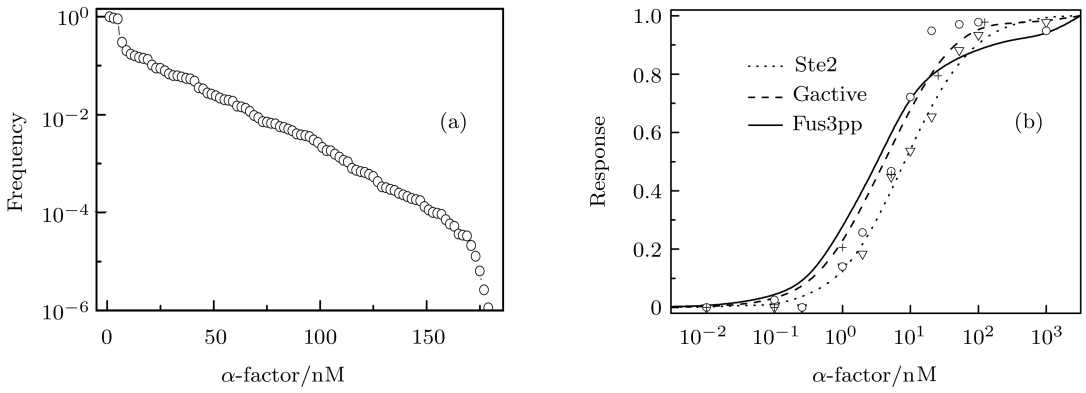


Fig.7. (a) The occurrence frequencies of the 185 reactions sorted in descending order showing wild differences in the times the reactions occur. The frequencies have been normalized to the maximal value. Parameters: α-factor = 10 nM, $\Omega = 8.0$. (b) Dose-response curves of the simplified network for key proteins in the mating pathway. Simulated results for activated Ste2 (dotted line), activated G protein (dashed line), and Fus3pp (full line) are in agreement with experimental data of down-triangles, circles, and crosses, respectively.

These most frequently fired reactions constitute the skeleton of the pathway. They play dominant roles and make the main body of the pathway. Simulations show that closing any one of the high-occurrence reactions will ruin the proper function of the pathway. It was reported that the dephosphorylation of kinases involved in the MAPK cascade and scaffold-dependent reactions play key roles in regulating the response to pheromone induction and in keeping the fidelity of the mating signalling.[12] Our stochastic simulations show that the reactions involved in these processes have top occurrence frequencies. Previous studies have found that the binding site of Fus3 for Ste5 binds Ste7,[24] i.e, Ste7 and Ste5 compete to bind Fus3, providing a buffering mechanism for regulating the abundance of free Fus3 and Ste7 in the cytosol. Our simulations find here that the association and decomposition of the complex Ste7·Fus3 occur also in very high frequencies, indicating that the buffering effect is key for the proper function of the mating pathway.

The reactions of high occurrence frequency take up only a small fraction of the reaction pool and a large portion of reactions in the network occur in low frequencies. Simulation shows that most of the low firing-frequency reactions are scaffold-dependent MAPK cascade reactions. In the module of MAPK cascade, as scaffold Ste5 has three binding sites respectively for Ste11(pp), Ste7(pp), and Fus3(pp) to form scaffold–kinase complexes, there are in total 27 possible kinds of scaffold–kinase complexes (C_i, $i = 1, 2, \ldots, 27$). As there is no experimental evidence for these complexes, we have considered all the possible 105 scaffold-dependent reactions in the model. Stochastic simulations reveal that only a small portion of 105 reactions occur frequently. Another group of reactions that have low occurrence frequency lies among those in the MAPK cascade in the cytosol, i.e., the phosphorylation of Ste7 to Ste7pp and Fus3 to Fus3pp. This provides more verification of the conclusion in Ref.[12] that the mating signal transduction is mainly fulfilled through the MAPK cascade on the Ste5 scaffold, and the mating pathway is highly scaffold dependent.

As a reaction that happens more often could generally be more likely to be important or contribute more to the signal transduction, we expect that the model we have simulated to be simplified by neglecting the reactions of low occurrence frequency. We managed to turn off in total 113 reactions that occur most rarely in the pathway and obtain a greatly simplified model. These closed reactions include R_5, $R_{11} - R_{14}$, R_{16}, R_{18}, $R_{27} - R_{29}$, $R_{33} - R_{35}$, $R_{39} - R_{41}$, $R_{45} - R_{47}$, $R_{55} - R_{61}$, R_{63}, $R_{65} - R_{74}$, R_{76}, $R_{78} - R_{88}$, R_{90}, $R_{93} - R_{102}$, $R_{104} - R_{114}$, R_{116}, $R_{118} - R_{120}$, $R_{122} - R_{124}$, $R_{126} - R_{130}$, $R_{132} - R_{138}$, $R_{140} - R_{144}$, $R_{146} - R_{152}$, $R_{154} - R_{156}$, R_{158}, R_{159}, R_{163}, R_{165}, R_{167}, R_{169}, R_{171}, R_{173}. There are 87 out of 105 reactions in the scaffold-dependent MAPK cascade that seem to be non-essential, and the cascade is reduced to several cyclic reaction loops that transform the scaffold–kinase complexes from one into another, i.e., two triangle cycles $C_{24} \rightarrow C_{27} \rightarrow C_{10} \rightarrow C_{24}$ and $C_{18} \rightarrow C5 \rightarrow C_{17} \rightarrow C_{18}$, two other larger loops $C_{13} \rightarrow C_{21} \rightarrow C_{24} \rightarrow C_{27} \rightarrow C_{14} \rightarrow C_3 \rightarrow C_{13}$, and $C_1 \rightarrow C_6 \rightarrow C_{12} \rightarrow C_{13} \rightarrow C_{21} \rightarrow C_{24} \rightarrow C_{27} \rightarrow C_{18} \rightarrow C_7 \rightarrow C_1$. There are also 12 MAPK reactions in the cytosol and other 14 reactions of low occurrence frequency neglected. We find that closing these 113 reactions of lowest occurrence frequency does not cause significant changes in the function of the pathway. The frequency distribution pattern of the new pathway resembles closely the original. As the sensitivity to the induction of different pheromone levels is an important feature of the signal transduction pathway, we have calculated the dose-response curves for the new simplified model. Figure 7 demonstrates that the response curves of the key components $\mathrm{Ste2_{active}}$, activated G protein (sum of Gα·GTP and Gα·GDP), and MAPK Fus3pp predicted by our simplified model still agree with experiments.[9,25] The results suggest that the greatly simplified model captures the essence of the original full model.

4. Summary and discussion

We have studied the yeast mating pheromone response pathway at system level by carrying out stochastic simulations for an individual or for a population of yeast. The stochastic temporal behaviour of the pathway is found to be robust to the influence of inherent fluctuations, and the intrinsic noise propagates in the pathway in a uniform pattern when the yeasts were treated with pheromone of different stimulus strengths and of varied fluctuations. The influence of extrinsic noise is found to be generally local when a single parameter was perturbed. The noise susceptibility of the pathway is enhanced when the signal transduction process is influenced by intrinsic noise in combination with external noise or cell-to-cell differ-

ence in the capacity of the pathway.

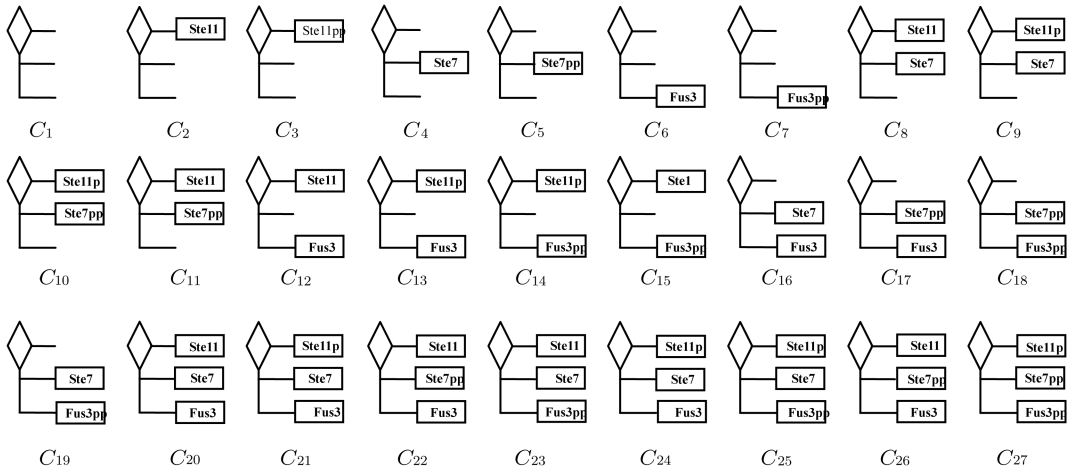
The influence of noise in the pathway on cell-to-cell variability has been studied in a recent experiment.[17] Quantitative measurements revealed that the cell-to-cell variation was dominated by the noisy capacity of individual cells to transmit signals and to express proteins from genes. We have tested the roles played by intrinsic and extrinsic noise in cell-to-cell variations in our stochastic simulations. By using an analogue of the experimental dual-reporter technique, we distinguish the intrinsic and extrinsic contributions to the total variation in the level of proteins in the pathway. In accordance with recent experimental findings, our simulations showed that extrinsic variability is more prominent, and only a small proportion of total cell-to-cell variation is caused by internal random fluctuations.

The occurrence frequency of a reaction is simply determined by protein abundance and rate constants. The reactions in the pathway were found to have a wide range of difference in their occurrence frequencies. A large portion of the reactions in the pathway were found to occur rarely, and the occurrence frequencies sorted in descending order fall exponentially. We found that closing most of the reactions that occur rarely did not cause significant changes in the temporal behaviour of the pathway. This is a manifestation of the robustness of the pathway. The dose-response curves obtained from the simplified network were found to agree qualitatively with the original model as well as with experimental data.[12] The reactions that occur often are key because they carry the majority of the reaction fluxes, i.e., the mating signal, in the pathway. Simulations show that closing any one of the high-occurrence reaction will ruin the proper function of the pathway.

It should be admitted that the model we adopt here has some limitations and might not represent fully the actual pathway. For instance, the model is fine grained on the protein complexes formed during the MAP kinase cascade of the signalling pathway, but very coarse on the complexes formed elsewhere. Due to lack of clear support from experimental data, the kinase and phosphatase reactions that happen in the cytoplasm were assumed to be distributed, and they were assumed to be processive when the kinases are bound to the scaffold Ste5. In addition, it was assumed that all scaffold is initially in the nucleus which is not consistent with available data. Despite the flaws in the model we simulated, the results we reported here might still be significant for the understanding of stochastic properties of general signalling pathways.

Appendix

The 27 scaffold–kinase complexes considered in our model for the yeast mating pathway, and reaction rate constants and initial conditions used in our stochastic simulation are listed in the following.



List of 27 types of scaffold–kinase complexes at the membrane. The diamond symbol at the upper-left corner indicates the G$\beta\gamma$Ste20 complex.

Table 1. Reaction constants applied in the stochastic model.

parameter	value	parameter	value
G-protein cycle:		downstream reactions:	
k_1	0.12 $nM^{-1} \cdot min^{-1}$	k_{28}	8 $nM \cdot min^{-1}$
k_2	0.6 min^{-1}	k_{29}	40 nM
k_3	0.24 min^{-1}	k_{30}	0.01 min^{-1}
k_4	320 $nM \cdot min^{-1}$	k_{31}	0.5 $nM \cdot min^{-1}$
k_5	7 nM	k_{32}	10 $nM \cdot min^{-1}$
k_6	30 $nM \cdot min^{-1}$	k_{33}	2 $nM \cdot min^{-1}$
k_7	0.024 min^{-1}	k_{34}	7 nM
k_8	0.0048 $nM^{-1} \cdot min^{-1}$	k_{35}	0.002 min^{-1}
k_9	115 $nM \cdot min^{-1}$	k_{36}	8 $nM^{-1} \cdot min^{-1}$
k_{10}	60 nM	k_{37}	1 min^{-1}
k_{11}	20 $nM \cdot min^{-1}$	k_{38}	10 min^{-1}
k_{12}	0.08 min^{-1}	k_{39}	10 min^{-1}
k_{13}	0.24 min^{-1}	k_{40}	0.1 $nM^{-1} \cdot min^{-1}$
k_{14}	0.025 $nM^{-1} \cdot min^{-1}$	k_{41}	0.01 min^{-1}
k_{15}	480 $nM^{-1} \cdot min^{-1}$	k_{42}	0.01 $nM^{-1} \cdot min^{-1}$
recruitment of scaffolds:		k43	0.1 min^{-1}
k_{16}	0.05 $nM^{-1} \cdot min^{-1}$	k_{44}	32 $nM \cdot min^{-1}$
k_{17}	5 min^{-1}	k_{45}	1 nM
k_{18}	0.00007 $nM^{-1} \cdot min^{-1}$	k_{46}	0.052 min^{-1}
k_{19}	0.001 min^{-1}	k_{47}	10 min^{-1}
k_{22}	0.3 min^{-1}	k_{48}	14 min^{-1}
k_{23}	30 min^{-1}	k_{49}	8 min^{-1}
some cytosol reactions:		k_{50}	15 min^{-1}
k_{24}	1.2 $nM^{-1} \cdot min^{-1}$		
k_{25}	24 min^{-1}		
k_{26}	0.0015 $nM^{-1} \cdot min^{-1}$		
k_{27}	0.1 min^{-1}		

Table 2. Constants for MAPK cascade in the cytosol. Reactions are all in the form: $S + E \underset{a_n}{\overset{d_n}{\rightleftharpoons}} SE \xrightarrow{p_n} S^* + E$. Subscripts 1, 2 in a_i, d_i, p_i denote dephosphorylation of once (such as Fus3p) and twice (such as Fus3pp) phosphorylated kinases respectively. Subscripts 3, 4 denote once and twice phosphorylation respectively.

dephosphorylations:						
protein	$a_1/(nM^{-1} \cdot min^{-1})$	d_1/min^{-1}	p_1/min^{-1}	$a_2/(nM^{-1} \cdot min^{-1})$	d_2/min^{-1}	p_2/min^{-1}
Ste11	0.5 (a_{1kkk})	24 (d_{1kkk})	10 (p_{1kkk})	1 (a_{2kkk})	24 (d_{2kkk})	10 (p_{2kkk})
Ste7	0.5 (a_{1kk}	24 (d_{1kk})	10 (p_{1kk})	0.5 (a_{2kk})	24 (d_{2kk})	10 (p_{2kk})
Fus3	0.2 (a_{1k})	10 (d_{1k})	30 (p_{1k})	0.4 (a_{2k})	20 (d_{2k})	30 (p_{2k})
Phosphorylations:						
protein	$a_3/(nM^{-1} \cdot min^{-1})$	d_3/min^{-1}	p_3/min^{-1}	$a_4/(nM^{-1} \cdot min^{-1})$	d_4/min^{-1}	p_4/min^{-1}
Ste7	0.5 (a_{3kk})	24 (d_{3kk})	10 (p_{3kk})	0.5 (a_{4kk})	24 (d_{4kk})	10 (p_{4kk})
Fus3	0.2 (a_{3k})	10 (d_{3k})	30 (p_{3k})	0.4 (a_{4k})	20 (d_{4k})	30 (p_{4k})

Table 3. Constants for binding (on) to and dislocation (off) from scaffold Ste5 for kinases, and their phosphorylation rates on Ste5. Symbol ** are for twice phosphorylated kinases.

protein	$on/(nM^{-1} \cdot min^{-1})$	off/min^{-1}	$**on/(nM^{-1} \cdot min^{-1})$	$**off/min^{-1}$	$phosphorylation/min^{-1}$
Ste11	1.2 (on_{kkk})	10 (off_{kkk})	1 (on_{2kkk})	10 (off_{2kkk})	20 (p_{kkk})
Ste7	1.2 (on_{kk})	0.1 (off_{kk})	–	0.5 (off_{2kk})	46 (p_{kk})
Fus3	1.2 (on_k)	10 (off_k)	–	200 (off_{2k})	250 (p_k)

Table 4. Initial protein abundances. The initial amounts for other proteins not listed here are all zeros.

protein	value/(nM)	protein	values
Ste2	1000	MAPKKK-P	100
Sst2	250	MAPKK-P	100
G protein	1000	MAPK-P_{in}	100
Ste20	1000	MAPK-p_{out}	100
Ste11	200	$Ste5_{in}$	125
Fus3Ste7	200	$Ste5_{out}$	0.1
Ste7	10	Cdc28	100
Fus_{in}	700	$Fus3_{out}$	300

References

[1] Dohlman H G and Thorner J W 2001 *Annu. Rev. Biochem.* **70** 703

[2] Bardwell L 2004 *Peptides.* **25** 1465

[3] Dohlman H G 2002 *Annu. Rev. Physiol.* **64** 129

[4] Gustin M C, Albertyn J, Alexander M and Davenport K 1998 *Microbiol. Mol. Biol. Rev.* **62** 1264

[5] Choi K, Satterberg B, Lyons D M and Eloin E A 1994 *Cell* **78** 499

[6] Kholodenko B N 2000 *Eur. J. Biochem.* **267** 1583

[7] Levchenko A, Bruck J and Sternberg P W 2000 *Proc. Natl. Acad. Sci. USA* **97** 5818

[8] Hao N, Yildirim N, Wang Y, Elston T C and Dohlman H G 2003 *J. Biol. Chem.* **278** 46506

[9] Yi T, Kitano H and Simon M 2003 *Proc. Natl. Acad. Sci. USA* **100** 10764

[10] Wang X, Hao N, Dohlman H G and Elston T C 2006 *Biophys. J.* **90** 1961

[11] Kofahl B and Klipp E 2004 *Yeast* **21** 831

[12] Shao D, Zheng W, Qiu W, Ouyang Q and Tang C 2006 *Biophys. J.* **91** 3986

[13] Raser J M and O'Shea E K 2005 *Science* **309** 2010

[14] Kaern M, Elston T C, Blake W J and Collins J J 2005 *Nature Reviews Genetics* **6** 451

[15] Rosenfield N, Young J W, Alon U, Swain P S and Elowitz M b 2005 *Science* **307** 1962

[16] Raser J M and O'Shea E K 2004 *Science* **304** 1811

[17] Colman-Lerner A, Gordon A, Serra E, Chin T, Resnekov O and Endy D 2005 *Nature* **437** 699

[18] Gillespie D 1977 *J. Phys. Chem.* **81** 2340

[19] Roberts C J, Nelson B, Marton M J, Stoughton R, Meyer M R and Bennett H A 2000 *Science* **287** 873

[20] Zeitlinger J, Simon I, Harbison C T, Hannett N M, Volkert T L and Fink G R 2003 *Cell* **113** 395

[21] Blue J L, Beichl I I and Sullivan F 1995 *Phys. Rev.* E **51** R867

[22] Scott M, Ingalls B and Kaern M 2006 *Chaos* **16** 026107

[23] Elowitz M B, Levine A J, Siggia E D and Swain P S 2002 *Science* **297** 1183

[24] Kusari A B, Molina D M, Sabbagh W, Lau C S and Bardwell L 2004 *J. Cell. Biol.* **164** 267

[25] Anderson J, Simpson D M, Qi M, Wang Y and Elion E A 2004 *J. EMBO.* **23** 2564